Eur. Phys. J. B **19**, 517–523 (2001)

THE EUROPEAN PHYSICAL JOURNAL B

EDP Sciences

Influence of the crystallite size on the phase transformation of yttria irradiated with swift heavy ions

S. Hémon[1], A. Berthelot[1,2], Ch. Dufour[2,a], F. Gourbilleau[2], E. Dooryhée[3], S. Bégin-Colin[4], and E. Paumier[2]

[1] CIRIL, CEA-CNRS-ISMRA, rue Claude Bloch, BP 5133, 14070 Caen Cedex 5, France
[2] LERMAT[b], ISMRA, 6 boulevard du Maréchal Juin, 14050 Caen Cedex, France
[3] ESRF, avenue des Martyrs, BP 220, 38043 Grenoble Cedex, France
[4] LSGMM[c], École des Mines, 54042 Nancy Cedex, France

Received 27 January 2000 and Received in final form 13 December 2000

Abstract. The irradiation effects induced by swift heavy ions are now widely described in 'bulk' materials. It is shown here that the behaviour of matter under irradiation depends on its crystalline state in the sense that a given material is all the more sensitive to swift heavy ion irradiations as the mean crystallite size L is small. The present paper relates the experimental results obtained in yttrium oxide from '*in situ*' X-ray diffraction measurements. Three kinds of sample have been irradiated: sintered samples ($L = 1$ μm), non-ground powders ($L = 45$ nm) and ground powders ($L = 28$ nm). A cubic to monoclinic phase transformation appears if the electronic energy loss of the incident particle is higher than a threshold. The comparison between the different kinds of samples reveals that this phase transformation is all the easier as the mean crystallite size of the target is weak.

PACS. 61.50.-f Crystalline state – 61.80.-x Physical radiation effects, radiation damage – 64.70.-p Specific phase transitions

Introduction

Since two decades, the effects of irradiation of matter with swift heavy ions have been extensively studied. Only recently, the growing interest of low dimensional materials (such as thin films or polycrystalline materials) led the scientific community to focus its attention on such targets [1–3]. Swift heavy ions such as those produced by GANIL (Grand Accélérateur d'Ions Lourds, Caen-France) have an energy of several MeV/u. Passing through the matter, they deposit the most part of their energy through inelastic collisions with the target electrons inducing for example amorphisation [4–6], recrystallisation [7] or phase change [8–11]. The spatial distribution of this energy deposition strongly depends on the ion velocity and has been theoretically studied: the energy density deposited near the ion path is all the higher as the ion velocity is weak [12]. The velocity effect has been experimentally demonstrated in 'bulk' materials whether they are metallic [13] or insulating [14]. Among insulators, yttrium oxide has been studied because several phases may exist according to temperature and pressure conditions: the normal phase is cubic whereas a monoclinic phase appears at high temperature and pressure. It has been previously demonstrated that this phase change occurs under irradiation with swift heavy ions [11,15].

The aim of this paper is to investigate the effect of the mean crystallite size of the target on the material response to irradiation. For this purpose, three kinds of yttrium oxide targets have been irradiated: i) sintered samples, ii) non ground powders and iii) ground powders. The mean crystallite size decreases from type i) to iii). The irradiation effect has been identified through X-ray diffraction measurements.

1 Experimental setup

The samples of yttrium oxide were irradiated with swift heavy ions at GANIL in Caen, France. The following ions were used: sulfur, molybdenum, cadmium, tantalum, and lead. Their energy varied between 3.1 and 11.1 MeV/u and their electronic stopping power S_e between 3 and 39 keV nm^{-1}. The irradiation features are given in Table 1.

The sintered samples were obtained from an yttrium oxide powder by Hot Isostating Pressing without any addition, at a temperature of 1400 °C and under a pressure of 150 MPa. The samples were irradiated with lead ions with two fluences: 2×10^{12} Pb cm^{-2} and 8×10^{12} Pb cm^{-2} and were then analyzed by powder X-ray diffraction before and after irradiation.

Yttrium oxide powders provided by Sigma Aldrich (Saint-Quentin Fallavier, France) have also been studied. The as-received powders are called in the following the *non-ground powders*. A series of samples are obtained by

[a] e-mail: dufour@labolermat.ismra.fr
[b] Unité CNRS associée n°6004
[c] URA CNRS 159

Table 1. Features of the different irradiations.

ion	energy (MeV/u)	electronic stopping power (keV nm^{-1})	Range (μm)	irradiated sample	maximal reached fluence (ions cm^{-2})
S	11.1	3	95	non ground powder	3.6×10^{13}
Mo	8.6	16	50	non ground powder	4.5×10^{13}
				ground powder	4.5×10^{13}
Cd	9.5	19	55	non ground powder	8.0×10^{12}
				ground powder	8.0×10^{12}
Ta	5.6	34	39	non ground powder	2.6×10^{13}
				ground powder	2.6×10^{13}
Pb	3.8	38	29	single crystal	8.0×10^{12}
				sintered sample	8.0×10^{12}
				non ground powder	4.2×10^{12}

ball-milling of the powder in a steel vial with seven steel balls (13 mm in diameter during 15 minutes [16]). In the following, these samples are called *the ground powders*. Several samples of non ground powder have been irradiated with sulfur, molybdenum, cadmium, tantalum and lead ions while samples of ground powder were irradiated with molybdenum, cadmium and tantalum ions (Tab. 1). The powders were pressed into pellets before irradiation. The samples were put into a 10^{-6} Torr vacuum chamber. They were submitted to several fluences at the end of which they were analyzed *in situ* with a powder X-ray diffractometer, using the INEL Curved Position Sensitive detector with the quartz-monochromated Cu Kα radiation. The sample are placed so that the surface normal is parallel to the ion beam while the X-ray beam is at 5°–10° incidence with respect to the sample surface. These conditions ensure that the penetration depth of the X-ray beam (estimated to 20 μm from the absorption coefficient $\mu = 442$ cm^{-1}) is lower than the ion range (35 μm in the worst case of a 5 MeV/u Pb ion). Along the ion path, the electronic stopping power varies from 38 keV nm^{-1} to 32 keV nm^{-1}. After each predetermined fluence, the ions are stopped. The sample holders are activated and exhibit a huge fluorescence so that no measurement is made before a 30 minutes pause is respected. Then the X-ray diffraction spectrum is recorded during 45 minutes. All the experiments have been performed at room temperature.

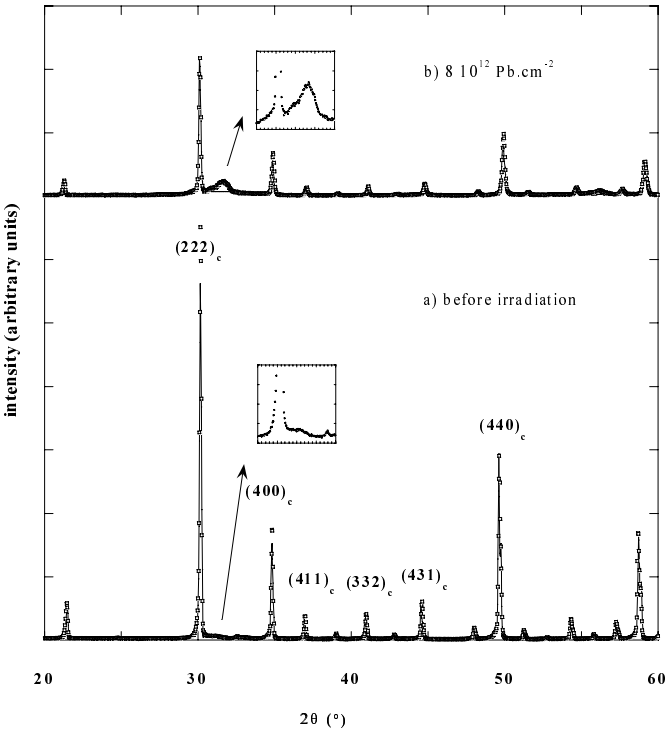

Fig. 1. Experimental (squares) and calculated (line) X-ray diffraction spectra of the sintered sample (a) before irradiation and (b) after the fluence 8×10^{12} Pb cm^{-2}. The insets correspond to a zoom in the range ($29° < 2\theta < 33°$).

2 The samples before irradiation

2.1 The sintered samples

The diffraction patterns observed in the virgin samples are displayed in Figure 1a. The samples later irradiated with lead ions exhibit diffraction spectra that show a small proportion of monoclinic Y_2O_3 – revealed by a 'shoulder' ($29° < 2\theta < 33°$) – within a mainly cubic phase.

The peak widths are close to those of the micrometric silicon powder (provided by INEL) which is used to calibrate the detector. The mean crystallite size of the sintered samples is thus assumed to be around 1 micrometer.

2.2 The non ground powder

The X-ray diffraction spectrum before irradiation is given in Figure 2a and corresponds to that of a 100% cubic phase yttrium oxide powder. A Gaussian profile is assumed for each peak: the experimental width B_e is linked to the

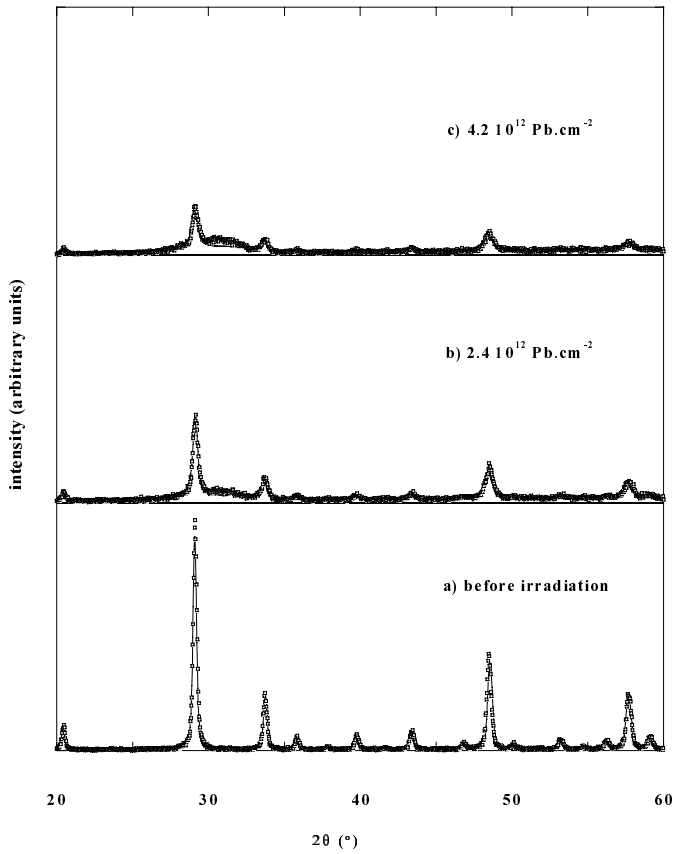

Fig. 2. Experimental (squares) and calculated (line) X-ray diffraction spectra of the non ground powder (a) before irradiation and after the fluences (b) 2.4×10^{12} Pb cm^{-2} and (c) 4.2×10^{12} Pb cm^{-2}.

width B due to the sole sample, and to the width B_i due to the instrument, by the relation: $B_\mathrm{e}^2 = B^2 + B_i^2$. Our apparatus has an instrumental width B_i equal to 0.12° determined with the aid of the calibrating silicon powder. The experimental one B_e deduced from the *cubic*-(400) peak at $2\theta = 33.9°$ is equal to 0.270°. Consequently, B is equal to 0.242° (*i.e.* 4.22×10^{-3} rad). The Scherrer formula gives the apparent size L of the crystallites using the relation ship $B = K\lambda/(L\cos\theta)$ where K is a constant close to the unity, λ the wavelength of the X-ray beam and θ the diffraction angle. L is found equal to 38 nm that is close to the size (45 nm) deduced from TEM observation (Fig. 3).

2.3 The ground powder

The ground powder is observed before irradiation by X-ray diffraction (Fig. 4a). The spectrum is that of a partly cubic powder but the shoulder between 29° and 33° proves the presence of the monoclinic phase before irradiation. The peaks of the cubic phase are wider than the ones of the non-ground powder. The experimental width is equal to $B_\mathrm{e} = 0.355°$, so $B = 0.34° = 5.83 \times 10^{-3}$ rad. The mean size of the crystallites, deduced from the Scherrer formula, is 28 nm. The main effect of grinding is to reduce the crystallite size.

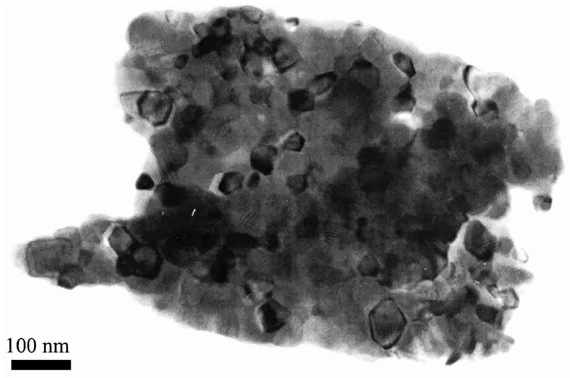

Fig. 3. Transmission Electron Microscopy picture of a non-ground Y_2O_3 powder.

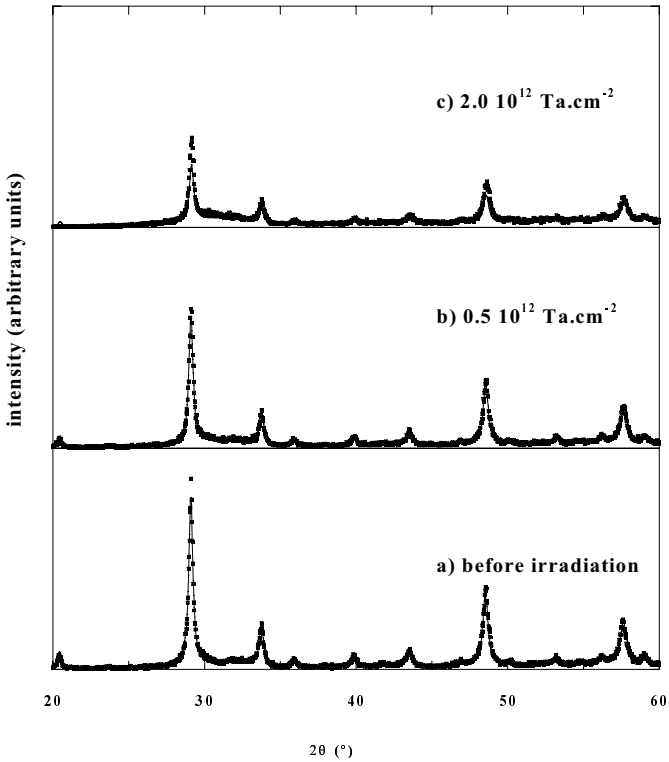

Fig. 4. Experimental (squares) and calculated (line) X-ray diffraction spectra of the ground powder (a) before irradiation and after the fluences (b) 0.5×10^{12} Ta cm^{-2} and (c) 2.0×10^{12} Ta cm^{-2}.

3 Irradiation experiments

3.1 Qualitative description of the X-ray diffraction spectra

3.1.1 Sintered samples

After irradiation with Pb ions, the height of each peak decreases with increasing fluence (Fig. 1). The experimental peak widths B_e seem to remain constant. This observation is due to the fact that the width B due to the sample is much lower than the instrumental one B_i ($B_\mathrm{i} = 0.12°$). Hence the variation of B cannot be observed as long as $B \ll B_\mathrm{i}$ (the relationship between B, B_e and B_i has been

explained in Sect. 2.2). The value of 0.01° is expected for B in the case of micrometric crystallites.

The surface of the shoulder in the region $29° < 2\theta < 33°$ increases with the fluence which proves that the proportion of the monoclinic phase increases with the fluence.

3.1.2 The non ground powder

Under sulfur ion irradiation ($S_e = 3$ keV nm^{-1}), the recorded X-ray spectra (not shown here) remain unchanged: no phase transition occurs.

For electronic stopping powers higher than 16 keV nm^{-1}, all the spectra show the same general features: a decrease of the height and an increase of the width of the cubic phase peaks are simultaneously observed when the fluence increases. This is the case of Mo ($S_e = 16$ keV nm^{-1}), Cd ($S_e = 19$ keV nm^{-1}), Ta ($S_e = 34$ keV nm^{-1}) and Pb ($S_e = 38$ keV nm^{-1}) irradiations. The typical spectra obtained at two different fluences after the lead irradiation are shown in Figure 2. In addition to the general features, a shoulder appears in the region $29° < 2\theta < 33°$ and grows with increasing fluence. This "shoulder" corresponds to the (111), (401) and (402) peaks of the monoclinic phase. The cubic to monoclinic phase transition is obtained under ion irradiation. Concerning the lighter ions (Mo and Cd), a more detailed analysis of the spectra is required to evidence this phase transition (see Sect. 3.3).

3.1.3 The ground powder

As written in Section 2.4, the virgin samples are composed of yttrium oxide with a mainly cubic structure in which a small fraction of the monoclinic phase is present as shown by the 'shoulder' in the $29° < 2\theta < 33°$ region of the spectra (Fig. 4).

After irradiation of such powders in the range of S_e between 16 and 39 keV nm^{-1}, the intensity of the cubic phase peaks decreases whereas the intensity of the 'shoulder' increases with increasing fluence, pointing out the growth of the monoclinic phase.

3.2 Analysis by Rietveld method

3.2.1 Principles of the method

The X-ray diffraction spectra are recorded as a function of the diffraction angle 2θ and analyzed by the Rietveld method improved in the Fullprof program [17]. The least mean square procedure has been used to fit the theoretical spectra to the experimental ones taking into account: i) the number of phases of the studied sample, ii) the background signal, which is a function of θ and iii) the temperature factors linked to the thermal motion of each kind of atom.

Each peak of the diffraction spectra is fitted by a pseudo-Voigt function (P) that is the weighted sum of a Lorentzian (L) and a Gaussian (G), according the relation: $P(2\theta) = \eta L(2\theta) + (1 - \eta)G(2\theta)$, where η is a parameter that may be varied.

The goodness of fit is given by the usual χ^2 value from which we evaluate the error bars. Nevertheless, we must be careful about the physical sense of the calculated parameters which may be numerous. For example, the lattice parameters must be found close (within a few percent) to the ones found in the literature [18,19] otherwise the results cannot be taken into account.

An important point arises concerning the 'background intensity' of the XRD spectra. In our experiments, the irradiation induces the fluorescence of yttrium oxide which leads to an increase of the background intensity depending on the time elapsed between the end of each irradiation cycle and the beginning of the X-ray spectra recording. That is the reason why no physical information can be extracted from the background signal.

The Rietveld analysis – used here – is based on the assumption that the cubic phase transforms into the monoclinic phase only. The self-consistency of this assumption will be shown in Section 4.2. Each phase present in the sample is characterized by the scale factor linked to its volume fraction, the lattice parameters a, b, c and the associated angles α, β, γ

The Rietveld analysis gives for each sample and each fluence the volume fraction f_c of the cubic phase. The volumic proportion f_b of the monoclinic phase will be taken equal to $[1 - f_c]$.

3.2.2 Evolution of the volume fraction of the cubic phase under irradiation

We did not attempt to fit the monoclinic phase parameters because i) the diffraction angles of the main lines of both phases (*i.e.* (222) cubic and (111) (401) (402) monoclinic) are almost the same and ii) the structure factors of the monoclinic phase are much lower than those of the cubic phase. The monoclinic phase parameters have been taken from reference [20]: $a = 14.009$ Å, $b = 3.500$ Å, $c = 8.791$ Å and $\beta = 95.7$. We have also fixed the temperature factors of each phase.

The parameters that have been varied in order to obtain the best fits are the scaling factor, the lattice parameters of the cubic phase and the parameters describing the background intensity.

The sintered samples:

Concerning the lead irradiation experiment, the volume fraction can be estimated to 7% in the unirradiated samples and reaches 15% and 46% after the fluences of 2.0×10^{12} Pb cm^{-2} and 8.0×10^{12} Pb cm^{-2}, respectively. The large errors bars (derived from high χ^2 values) can be explained by the fact that the Rietveld analysis is normally used for 'ideal' powders containing large and randomly orientated crystallites so that line breadths are very small. In the sintered samples, the crystallites are probably not randomly orientated. In fact, a preferred orientation is detected when the relative intensities in the measured spectrum do not follow the corresponding ones in

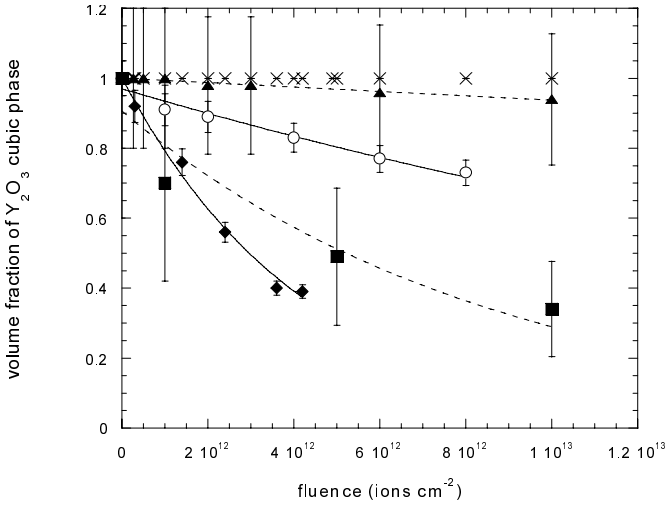

Fig. 5. Evolution of the volume fraction of the cubic phase of non ground Y_2O_3 *versus* the fluence for the irradiations with S (⋆), Mo (▲), Cd (○), Ta (■), Pb(♦). The lines correspond to the exponential fit.

the recorded JCPDS file: that is the case of the sintered samples.

The non-ground powders

All the samples are totally crystallized in the cubic phase before irradiation (*i.e.* $f_{c0} = 1$). Figure 2 shows that the calculated spectra well fit the experimental ones in the case of lead irradiation. The goodness of fit is noticed for all the irradiations. Each irradiation (Mo, Cd, Ta and Pb) gives the same feature shown in Figure 5: the volume fraction f_c of the cubic phase decreases with increasing fluence. A cubic to monoclinic phase transformation occurs under irradiation. The ions with the highest electronic stopping powers ($S_e > 34$ keV nm^{-1} for Ta and Pb) are more efficient than the ones with low S_e values ($S_e < 20$ keV nm^{-1} for Mo and Cd).

Within each irradiation experiment, the relative variation of the cubic phase lattice parameter given by the Rietveld refinements is of the order of 0.3%. It must be noticed that the instrumental breadth is 0.12° (for $2\theta = 29°$) so that the minimum measurable variation of the lattice parameter a is $\frac{\Delta a}{a} = 0.8\%$. Hence, we can consider that the lattice parameter a of the cubic phase does not change under irradiation.

The ground powders

Figure 4 shows a good agreement between calculated and experimental spectra in the case of the tantalum irradiation. As in the case of non-ground powders, the same goodness of fit is confirmed in all the irradiations.

On contrary to the other samples, the Rietveld analysis confirms the presence of the monoclinic phase before irradiation: the initial volumic proportion of monoclinic phase is about 20% so that $f_{c0} = 0.8$. The volume fraction f_c of the cubic phase decreases with increasing fluence. The cubic to monoclinic phase transformation is also evidenced and is made easier than in the non-ground powders.

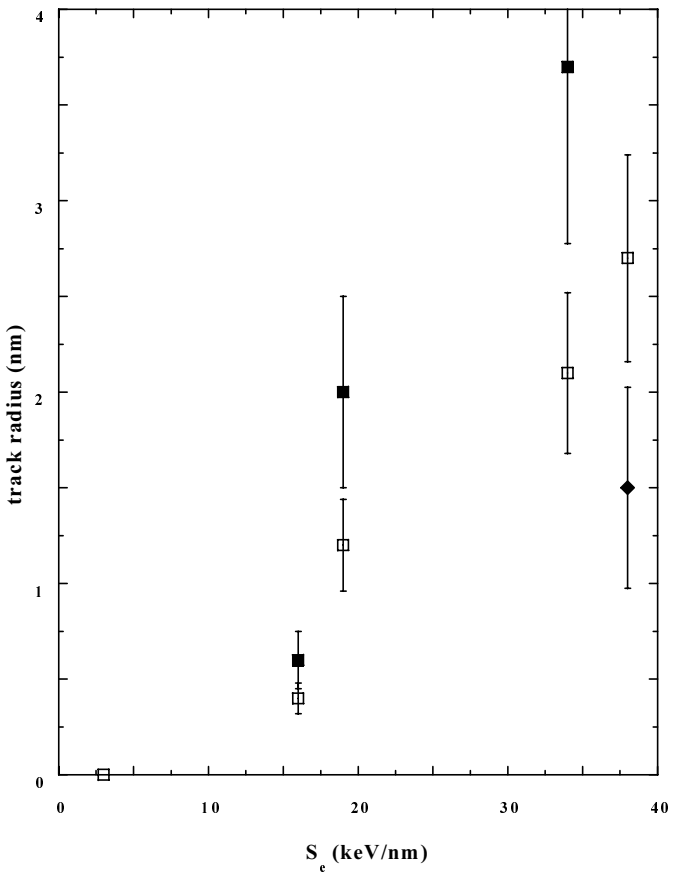

Fig. 6. Track radii in the sintered samples (diamonds), in the non ground powder (open squares) and in the ground powder (black squares) of Y_2O_3 *versus* the electronic stopping power S_e of the ions.

3.2.3 Track radii

In order to interpret the evolution of f_c *versus* the fluence ϕt, it is considered that, in a cylindrical zone of section σ along the ion path, the initial cubic phase is transformed into the monoclinic one. This section σ depends on the mean crystallite size L and on the presence of monoclinic nuclei as will be seen in Section 4. For a given type of sample (*i.e. a given value of L and a given monoclinic nuclei concentration*) Poisson's statistics is applied and it is found that the volume fraction f_c of the cubic phase after the passage of Φt ions per cm^2 is described by the relation: $f_c = f_{c0} \exp(-\sigma \Phi t)$. f_{c0} is the initial value of f_c before irradiation ($\Phi t = 0$). f_{c0} is lower than the unity when monoclinic nuclei are present which is the case of the ground powders. Each type of sample will exhibit a specific section σ.

Figure 5 shows the fit to this exponential law for each irradiation in the case of non- ground powders. The track radius r is linked to σ *via* the relation $\sigma = \pi r^2$ The same analysis is made for the sintered samples and the ground powders. Figure 6 shows the track radii variation *versus* the electronic stopping power for each kind of sample.

4 Discussion

4.1 Comparison of the results

In the case of the powders (either they are ground or not) three comments can be made:

a) the phase transformation occurs above of a S_e threshold between 5 and 15 keV nm^{-1}

b) the track radii increase with S_e.

c) the track radii observed in the ground powders are higher than those in the non-ground powders.

The results of the Rietveld analysis must be carefully interpreted in the case of the sintered samples since this method has been developed for powders in which the crystallites are randomly orientated. However, it appears that the deduced track radii are lower than those of powders.

Waligorski *et al.* [21] performed Monte Carlo calculations describing the radial dependence of the energy density $D(r)$ deposited by a swift ion on the electrons of a target.

The $D(r)$ law was confirmed several years later by Gervais *et al.* [22]. The mean energy density $\langle D(R)\rangle$ deposited within a cylinder of radius R is given by $\langle D(R)\rangle = \frac{1}{\pi R^2}\int_{r=0}^{R} D(r)2\pi r dr$. $\langle D(R)\rangle$ is plotted in Figure 7 for two ion energies (3 MeV/u and 11 MeV/u) corresponding to the energy range of the ions used in the present study and for an electronic stopping power of 30 keV nm^{-1}.

In the large crystallites of the sintered samples (R = 1 μm), $\langle D(R)\rangle$ is lower than 10^{-4} keV nm^{-1} whereas in the smaller grains of the powders (R = 30 nm) $\langle D(R)\rangle = 10^{-2}$ keV nm^{-1}. It is therefore likely that the smaller grains are more sensitive than the larger ones to the passage of the same ion. A clear size effect is evidenced through the study of the three kinds of samples.

Consequently, the phase transition induced in the material by the passage of the ion is easier in the non-ground powder than in the sintered sample.

We compare now the results between the two kinds of powders. Whatever the electronic stopping power of the ion, the track radius is higher in the ground powders than in the non ground ones. Two reasons may be found for explaining this behavior. First, the mean size of the crystallites has decreased by grinding the powder. So, for the reason explained above, the phase transition is easier in the ground powder than in the non ground powder. Second, the monoclinic phase is present before irradiation in the ground powder. The cubic to monoclinic phase transition occurs all the more easily, as some monoclinic seeds are present.

4.2 Does some amorphous phase appear under irradiation in the samples?

In principle, the Rietveld method cannot account for the presence of an amorphous phase. The input files contain the characteristics of both cubic and monoclinic phases so that the volume fractions f_c and f_b of each phase can be obtained. Let V_b and V_c be the volumes of the monoclinic and cubic phases respectively. Therefore the volume fractions f_b and f_c are given by: $f_b = \frac{V_b}{V_b+V_c}$ and $f_c = \frac{V_c}{V_b+V_c}$. The problem of the presence of an amorphous phase may be solved by comparing the Rietveld method to the intensity method described hereafter, under the following assumptions: i) the sample of volume V_{co} is initially wholly cubic and ii) the total volume remains constant under irradiation. The intensity method consists in determining the ratio I/I_0 as a function of the fluence ϕt. I is the sum of the intensities (*i.e.* the net areas) of the (222), (440) and (400) cubic phase peaks at the fluence ϕt and I_0 is the corresponding value before irradiation. Figure 8 shows the evolution of I/I_0 (open symbols, intensity method) and f_c (full symbols, Rietveld method) as a function the fluence ϕt in the case of three irradiations (Cd (squares), Ta (triangles) and Pb (circles)). In any case the ratio I/I_0 is equal to the volume fraction $f_c = V_c/V_{co}$ of the cubic phase. It is then proved that no amorphous phase appears within the experimental errors.

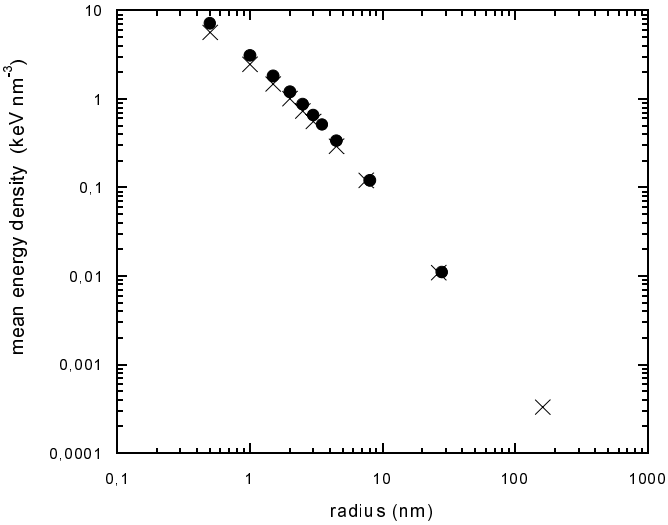

Fig. 7. Mean energy density (keV nm^{-3}) deposited on the electron of a grain of radius r (nm) in the case of two incident ion energies (3 MeV/u (crosses) and 11 MeV/u (black circles)). The calculation is performed for an electronic stopping power of 30 keV nm^{-1}.

Conclusion

The damage induced by swift heavy ions in yttrium oxide is characterized by a cubic to monoclinic phase transition. We have irradiated three kinds of samples of yttrium oxide: sintered samples, ground and non ground powders. We have evidenced an effect of the size of the crystallites of the sample: i) the sintered samples are not sensitive or weakly sensitive to the electronic stopping power; ii) the non ground powders transform easier than the sintered samples into the monoclinic phase; iii) this transition appears more clearly in the ground powder. Furthermore,

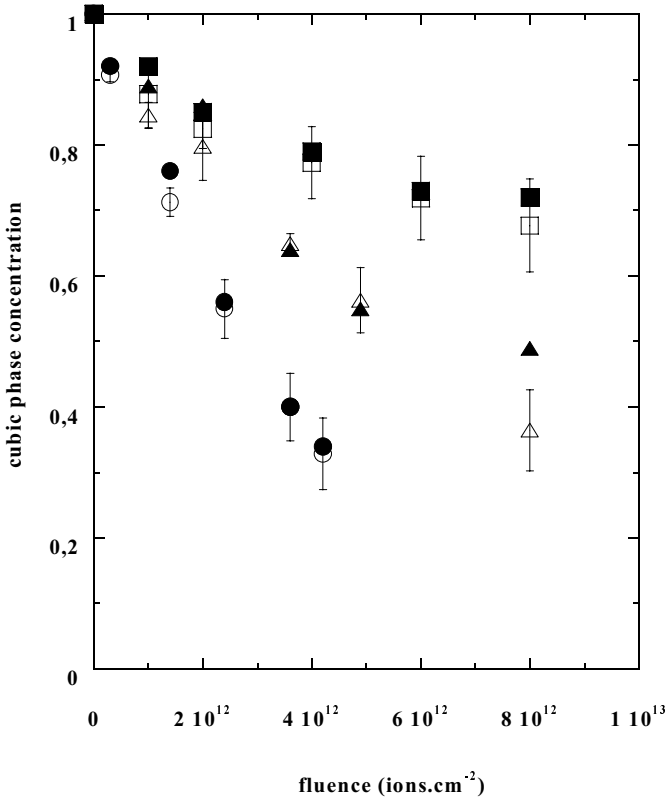

Fig. 8. Evolution of the cubic phase volume fraction as a function the fluence ϕt in the case of three irradiations (Cd (squares), Ta (triangles) and Pb (circles)). Comparison between the intensity method I/I_0 (open symbols) and the Rietveld method f_c (full symbols).

we have also proved that the initial volumic proportion of cubic phase is important: when the monoclinic phase is present before irradiation, the phase transition is easier. Finally, the phase transition that appears above a S_e threshold, is all the more important as the electronic stopping power of the ions increases: for the powders, this threshold has been found between 5 and 15 keV nm^{-1}.

The authors are grateful to F. Levesque (Centre Interdisciplinaire de Recherches Ions-Laser, Caen, France) for having provided technical support concerning the X-Ray powder diffractometer (CHEXPIR device).

References

1. S.M.M. Ramos, S. Bouffard, B. Canut, S. Della-Negra, M. Toulemonde, Nucl. Instrum. Methods Phys. Res. Sect. B **146**, 1 (1998).
2. F. Pawlak, Ch. Dufour, A. Laurent, E. Paumier, J. Perrière, J.P. Stoquert, M. Toulemonde, Nucl. Instrum. Methods Phys. Res. Sect. B **151**, 1 (1999).
3. S. Hébert, M. Hervieu, V. Hardy, T. Aouaroun, Ch. Simon, J. Provost, E. Milani, C. Aruta, G. Balestrino, Nucl. Instrum. Methods Phys. Research Sect. B **142**, 319 (1998).
4. D. Lesueur, Rad. Eff. Def. Solids **24**, 101 (1975).
5. A. Audouard, E. Balanzat, S. Bouffard, J.C. Jousset, A. Chamberod, A. Dunlop, D. Lesueur, G. Fuchs, R. Spohr, J. Vetter, L. Thomé, Phys. Rev. Lett. **65**, 875 (1990).
6. M. Toulemonde, J.M. Costantini, Ch. Dufour, A. Meftah, E. Paumier, F. Studer, Nucl. Instr. Meth. B **116**, 37 (1996).
7. K. Izui, S. Furuno, *Proc. XI* th *Int. Congr. On Electron Microscopy Kyoto, 1299 (1986)*, edited by T. Imura, S. Maruse, T. Suzuki (The Japanese Society of Electron Microscopy).
8. A. Dunlop, P. Legrand, D. Lesueur, N. Lorenzelli, J. Morillo, A. Barbu, S. Bouffard, Europhys. Lett. **15**, 765 (1991).
9. A. Dunlop, D. Lesueur, Rad. Eff. Def. Solids **126**, 123 (1993).
10. A. Dunlop, D. Lesueur, P. Legrand, H. Dammak, Nucl. Instr. Meth. B **90**, 430 (1994).
11. S. Hémon, V. Chailley, E. Dooryhée, Ch. Dufour, F. Gourbilleau, F. Levesque, E. Paumier, Nucl. Instr. Meth. B **122**, 563–565 (1997).
12. M.P.R. Waligorski, R.N Hamm., R. Katz, Nucl. Tracks Rad. Meas. **11**, 309 (1986).
13. Z.G. Wang, Ch. Dufour, B. Cabeau, J. Dural, G. Fuchs, E. Paumier, F. Pawlak, M. Toulemonde, Nucl. Instr. Meth. B **107**, 175 (1996).
14. A. Meftah, F. Brisard, J.M. Costantini, M. Hage Ali, J.P. Stoquert, F. Studer, M. Toulemonde, Phys. Rev. B **48**, 920 (1993).
15. S. Hémon, Ch. Dufour, F. Gourbilleau, E. Paumier, E. Dooryhée, S. Bégin-Colin, Nucl. Instr. Meth. B **146**, 443 (1998).
16. S. Begin-Colin, G. Le Caër, M. Zandona, E. Bouzy, B. Malaman, J. Alloys Comp. **227**, 157 (1995).
17. H.M. Rietveld, J. Appl. Cryst. **2**, 65 (1969).
18. JCPDS International Centre for Diffraction Data, card 25-1200.
19. H.R. Hoekstra, K.A. Gingerich, Inorg. Chem. **3**, 711 (1964) and Science **146**, 1163 (1964).
20. A.E. Solov'eva., Neorg. Mater. **21**, 808 (1985).
21. M.P.R. Waligorski, R.N. Hamm, R. Katz, Nucl. Tracks Meas. **11**, 309 (1987).
22. B. Gervais, S. Bouffard, Nucl. Instr. Meth. B **88**, 355 (1994).